PERGAMON

Scripta Materialia 45 (2001) 293–299

Scripta MATERIALIA

www.elsevier.com/locate/scriptamat

Prediction of yield stress for polysynthetically twinned TiAl crystals

Jun Yang[a], Gengkai Hu[a*], and Yonggang Zhang[b]

[a]*Department of Applied Mechanics, Beijing Institute of Technology, Beijing 100081, China*

[b]*Department of Material Science and Engineering, Beijing University of Aeronautics and Astronautics, Beijing 100083, China*

Received 2 November 2000; accepted 2 April 2001

Keywords: Yield stress; Lamellar structure; TiAl; Micromechanics; Modelling

Introduction

TiAl based alloys have good resistance to oxidation, creep and fatigue, and are considered to be one of the most promising structural materials for elevated temperature applications [1–3]. Polysynthetically twinned (PST) TiAl crystals, which consist of a series of well-oriented lamellae of TiAl (γ) and Ti_3Al (α_2), have been extensively used as a model material to study mechanical behavior of the lamellar microstructure. The mechanical properties of the PST crystal depend significantly on the lamellar orientation defined by the angle between the lamellae and the loading axis θ [4]. When $\theta = 0°$ or 90°, usually referred to as hard deformation modes, the PST crystals have the highest yield stress. In this case, dislocations have to overcome the interface barriers. When $\theta = 45°$, on the other hand, the motion of dislocations is relatively easy and the crystal has a low yield stress, corresponding to a soft deformation mode. The variation of the yield stress as a function of θ was determined experimentally by Fujiwara et al. [5]. Lebensohn et al. [6] adopted a pair of the matrix and the twin as a basic element, and proposed a method to evaluate the yield stress of PST crystals. Grujicic and Zhang [7] proposed a finite element method incorporating dislocation theory to analyze the yield and deformation of TiAl polycrystals. Kad et al. [8,9] studied the plastic deformation and fracture of PST crystals by numerical simulation and a micro-mechanical method. Sun [10] advanced a dislocation pile-up model to study the influence of the layer

* Corresponding author.
E-mail address: hugeng@public.bta.net.cn (G. Hu).

PII: S1359-6462(01)01030-2

thickness and the grain size on the yield behavior of an idealized TiAl polycrystal. Schlogl and Fischer [11] presented a micromechanical model and gave the simulation of the yield loci for PST crystals, and the detailed domain structures of the γ phase were considered with the help of finite element method.

In this paper, we will propose an analytical method based on dislocation theory and continuum micromechanics to predict the yield stress of a PST crystal as a function of the loading angle θ. The domain structures of the γ phase will be taken into account in an approximate analytical manner.

Microstructures of PST crystals

The PST crystal consists of the parallel plates of the γ phase and the interspersed α_2 phase, which is schematically shown in Fig. 1. The crystallographic orientation between the two phases is well known as $\langle 11\bar{2}0\rangle_{\alpha_2}\|\langle 1\bar{1}0\rangle_{\gamma}$ and $\{0001\}_{\alpha_2}\|(111)_{\gamma}$, with the $(111)_{\gamma}$ plane being parallel to the interfaces of the PST crystal. In the lamellar morphology, there are six possible orientations of $[110]_{\gamma}$ with respect to $\langle 1120\rangle_{\alpha_2}$, therefore the γ lamella is constituted by the ordered domain structures composed of six differently oriented variants γ_1, γ_2, γ_3, γ_4, γ_5, γ_6. In addition to α_2/γ interface, three different types of γ/γ interfaces with different interfacial structures are present, and each can be recovered by rotating 60° about $[111]_{\gamma}$ from its neighbor. The adjacent lamellae match exactly and have a $(111)[11\bar{2}]$ true twin orientation when the rotation is 180°. In the case of 60° rotation, the matching is only approximate and the neighborhood lamellae form a pseudo-twin. The detailed description of the PST structure can be found in Refs. [1,2,12].

In the following modeling, idealization of the PST crystal and the γ phase are illustrated by Figs. 1 and 2, respectively.

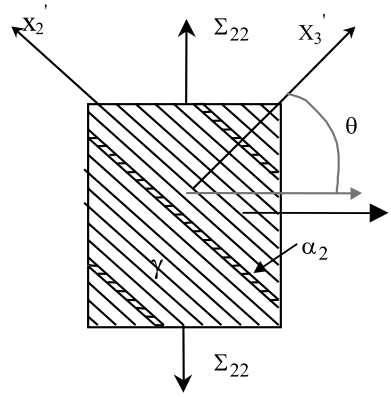

Fig. 1. Model of PST crystal.

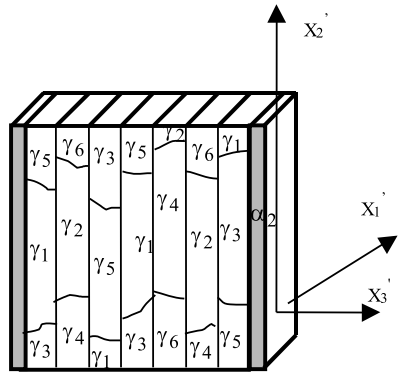

Fig. 2. Idealization of the microstructure of γ phase.

Micromechanical analyses

Modulus of PST crystal and average stress in the γ phase

In this section, the effective modulus of the PST crystal will be determined from its phase properties, and the distributed stresses in the different variants of the γ phase will be evaluated. To this end, the PST crystal is considered to be a composite material with the α_2 plates dispersed in the γ phase matrix. Since there are six differently oriented variants in the γ phase (Fig. 2), it is necessary to evaluate the average modulus of the γ phase material. The variants of the γ phase are transversely isotropic with x_3' being the symmetric axis (Fig. 2). Because all of the γ/γ interfaces are parallel to the plane $(1\,1\,1)_\gamma$, the average modulus of the γ-phase can be calculated by the orientation average of the six differently oriented variants $(\gamma_1, \gamma_2, \gamma_3, \gamma_4, \gamma_5, \gamma_6)$ in the plane $(1\,1\,1)_\gamma$. As a result, the average modulus of the γ phase is also transversely isotropic with the symmetric axis perpendicular to the plane $(1\,1\,1)_\gamma$, the same as the α_2 phase. The material constants for the variants of the γ phase and the α_2 phase are taken from the calculation performed by Yoo et al. [12], and are given together with the average modulus of the γ phase in the Table 1.

The PST crystal as a whole is also transversely isotropic with the same symmetric axis as the γ phase or α_2 phase. If the compliance tensors of the α_2 phase, the homogenized γ phase, and the PST crystal are denoted by $\mathbf{M}^I, \mathbf{M}^m$ and $\mathbf{M}$, respectively, it has [13]

$$\mathbf{M} = \mathbf{M}^m + f[(\mathbf{M}^I\mathbf{M}^{m^{-1}} - \mathbf{I})^{-1} + (1-f)(\mathbf{I}-\mathbf{S})]^{-1}\mathbf{M}^m \tag{1}$$

Table 1
Materials constants (unit: GPa)

Material constants	C_{11}	C_{33}	C_{12}	C_{13}	C_{44}
Variant of γ phase	190	185	105	90	120
α_2 phase	221	238	71	85	69
Average modulus of γ phase	237	251	77	63	130

where f is the volume fraction of the α_2 plates, **I** is unit tensor, **S** is Eshelby tensor, and $[\ ]^{-1}$ denotes the inverse of the said quantity.

In the following, the α_2 plates are considered as penny-shape inclusions dispersed in the homogenized γ phase. For a penny-shape inclusion in a transversely isotropic matrix, the Eshelby tensor can be written as in Wapole's notation [14]:

$$\mathbf{S} = \left[0\,0\ -M_{13}^m/(M_{11}^m + M_{12}^m)\ 1\,1\,0\right]$$

where M_{ij}^m are the components of the compliance for the homogenized γ phase.

The average stress in the homogenized γ phase is determined by [13]:

$$\langle \underline{\underline{\sigma}} \rangle_m = \frac{1}{1-f}(\mathbf{M}^m - \mathbf{M}^I)^{-1}(\mathbf{M} - \mathbf{M}^I)\underline{\underline{\Sigma}} = \mathbf{P} : \underline{\underline{\Sigma}} \tag{2}$$

where $\langle\ \rangle_m$ denotes the volume average over the matrix of the said quantity, $\underline{\underline{\Sigma}}$ is the applied macroscopic stress. In Wapole's notation, the effective compliance of the PST crystal is written as $\mathbf{M} = [\,c' \quad g' \quad g' \quad d' \quad e' \quad p'\,]$ with

$$c' = \frac{(M_{11}^I + M_{12}^I)(M_{11}^m + M_{12}^m)}{(1-f)(M_{11}^I + M_{12}^I) + f(M_{11}^m + M_{12}^m)}$$

$$g' = \frac{(1-f)(M_{11}^I + M_{12}^I)M_{13}^m + fM_{12}^m M_{13}^I}{(1-f)(M_{11}^I + M_{12}^I) + f(M_{11}^m + M_{12}^m)}$$

$$d' = fM_{33}^I + \frac{(1-f)\{f[2(M_{13}^I - M_{13}^m)^2 + M_{33}^m(M_{11}^I + M_{12}^I - 2M_{12}^m)] - (M_{11}^I + M_{12}^I)M_{33}^m\}}{(1-f)(M_{11}^I + M_{12}^I) + 2fM_{12}^m}$$

$$e' = fM_{44}^I + (1-f)M_{44}^m$$

$$p' = \frac{(M_{11}^I - M_{12}^I)(M_{11}^m - M_{12}^m)}{f(M_{11}^m - M_{12}^m) + (1-f)(M_{11}^I - M_{12}^I)}$$

The stress concentration tensor **P** and the average stress of the homogenized γ matrix under any external stress can be evaluated from Eqs. (1) and (2).

Analysis of yield stress for PST crystals

As shown in Fig. 1, in the global coordinate system, a tensile stress Σ_{22} is applied parallel to x_2, which can be written as $\underline{\underline{\Sigma}} = \{0 \quad \Sigma_{22} \quad 0 \quad 0 \quad 0 \quad 0\}^{\mathrm{T}}$, θ is the angle between Σ_{22} and X_2', and X_2' is parallel to the α_2/γ interface. It should be noted that in the interfacial plane $(1\,1\,1)_\gamma$, when $\theta = 0°$, either direction $[1\,1\,\bar{2}]_\gamma$ or $[1\,\bar{1}\,0]_\gamma$ may be arranged parallel to the loading direction, so in the following, these two possibilities will

be examined. The applied stress in the global system $x_1x_2x_3$ now is transformed to the local $X_1'X_2'X_3'$ coordinate system, this leads to

$$\underline{\underline{\Sigma}}' = \{\, 0 \quad \Sigma_{22}\cos^2\theta \quad \Sigma_{22}\sin^2\theta \quad -\Sigma_{22}\cos\theta\sin\theta \quad 0 \quad 0 \,\} \tag{3}$$

For the considered PST crystal, the slip directions of the variants γ_2, γ_3, γ_4, γ_5, γ_6 can be derived from those of the variant γ_1 by multiplying a transformation matrix such as $\{\gamma_i\} = [\mathrm{T}_i]\cdot\{\gamma_1\}$,

$$[\mathrm{T}_i] = \begin{bmatrix} \cos(i\cdot 60^\circ) & \sin(i\cdot 60^\circ) & 0 \\ -\sin(i\cdot 60^\circ) & \cos(i\cdot 60^\circ) & 0 \\ 0 & 0 & 1 \end{bmatrix} \tag{4}$$

In the previous subsection, the average stress in the homogenized γ matrix was evaluated. In order to analyze the slip characteristic of the variants, however, the stress distributed in each variant must be determined. Owing to the presence of the ordered domains in the γ lamellae, it is impossible to determine these distributed stresses in an exact manner. In the following, therefore, only two limit situations are considered: (1) all variants in the γ phase have a constant and equal stress, referred to as Reuss estimation; (2) all variants in the γ phase have a constant and equal strain, referred to as Voigt estimation.

The average stress $\langle\underline{\underline{\sigma}}\rangle_m$ and the average strain $\langle\underline{\underline{\varepsilon}}\rangle_m$ in the homogenized γ matrix were already determined in the previous sub section. According to Reuss estimation, the stresses in each variant of the γ matrix are given by $\underline{\underline{\sigma}}_{\gamma i} = \langle\underline{\underline{\sigma}}\rangle_m$, $(i = 1\text{–}6)$; and the stresses in the variants is $\underline{\underline{\sigma}}_{\gamma i} = \mathbf{C}_{\gamma i} : \langle\underline{\underline{\varepsilon}}\rangle_m$ if Voigt estimation is adopted, where $\mathbf{C}_{\gamma i}$ is the stiffness tensor of the γ phase in the global coordinate system for the ith variant.

If the normal vector of the slip plane is denoted by $\underline{n}$, and $\underline{l}$ denotes the slip direction, the resolved shear stress can be evaluated by $\tau = (\underline{\underline{\sigma}}_{\gamma i}\cdot\underline{n})\cdot\underline{l}$. The yield stress of the PST crystal is defined locally by the realization of Schmid criterion $\tau = \tau_{\mathrm{cr}}$ in any slip systems, this enables one, together with the previous micromechanical analysis, to determine the yield stress of the PST crystal as a function of the loading angle θ.

Fig. 3a and b illustrate the computed yield stresses as a function of the loading angle θ for the following two situations: (a) X_2' axis is initially parallel to $[1\,1\,\bar{2}]$; (b) X_2' axis is initially parallel to $[1\,\bar{1}\,0]$. The computed yield stresses in Fig. 3a and b are normalized by the yield stresses at $\theta = 90^\circ$ evaluated by each method, respectively, and the comparison with the experimental measurement [5] is also included in the figures.

It can be seen that Voigt estimation (constant strain in the variants) correlates well with experiment, and predicts more significant variation of the yield stress as a function of the loading angle θ compared to Reuss estimation. The initial loading orientations $[1\,\bar{1}\,0]$ or $[1\,1\,\bar{2}]$ have a minor influence on the final predicted result.

Table 2 gives the slip or twin systems when the critical external load is reached for the different angles θ for the case of loading direction parallel to $[1\,1\,\bar{2}]$.

The anisotropic behavior of the yield stress of PST crystals was usually explained on the basis of the interactions between the slips and the interfaces or the α_2 plates. For specimens with $0^\circ < \theta < 90^\circ$, shear deformation on $\{1\,1\,1\}_\gamma$ planes parallel to the

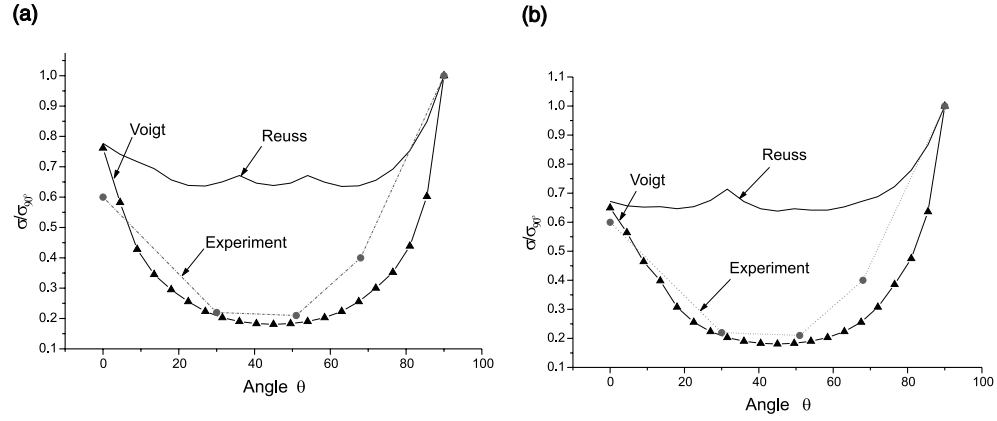

Fig. 3. Yield stress of PST crystal as function of loading angle θ: (a) tension in $[1\,1\,\bar{2}]$, (b) tension in $[1\,\bar{1}\,0]$.

Table 2
Primary slip or twin systems at different angle θ

θ	Slip system
0	$\gamma_1(\bar{1}\,1\,1)[0\,\bar{1}\,1]$, $\gamma_2(1\,1\,\bar{1})[\bar{1}\,1\,0]$, $\gamma_3(1\,\bar{1}\,1)[\bar{1}\,0\,1]$, $\gamma_4(\bar{1}\,1\,1)[0\,\bar{1}\,1]$, $\gamma_5(1\,1\,\bar{1})[\bar{1}\,1\,0]$, $\gamma_6(1\,\bar{1}\,1)[\bar{1}\,0\,1]$
$\pi/4$	$\gamma_1(1\,1\,1)[1\,1\,\bar{2}]$, $\gamma_4(1\,1\,1)[1\,1\,\bar{2}]$
$\pi/2$	$\gamma_1(1\,1\,\bar{1})[1\,1\,2]$, $\gamma_2(1\,1\,\bar{1})[1\,1\,2]$, $\gamma_3(1\,1\,\bar{1})[1\,1\,2]$, $\gamma_4(1\,1\,\bar{1})[1\,1\,2]$, $\gamma_5(1\,1\,\bar{1})[1\,1\,2]$, $\gamma_6(1\,1\,\bar{1})[1\,1\,2]$

lamellar interfaces in γ plates is always preferred, because the critical resolved shear stress for the slip systems in γ-TiAl is lower than that for the slip systems in α_2-Ti_3Al [15,16], and there is no barriers on the way for such a slip. Loading parallel or perpendicular to the lamellar planes causes slip and/or deformation twinning to occur on $\{1\,1\,1\}_\gamma$ planes across the lamellae. In such cases, the lamellar interfaces act as an effective barrier against propagation of the slip and/or twin through the interfaces. That is why the yield stress for the specimens loaded parallel or perpendicular to the lamellar interfaces is much higher than those for specimens loaded at intermediate angles of $0° < \theta < 90°$.

The fact that Voigt estimation gives better prediction than Reuss estimation seems to be supported by the experimental observation effectuated by Kashida et al. [17]. They concluded that strain continuity at domain and lamellar interfaces are one of the most important factors in determining the yield stress of PST crystals. In our modeling, Voigt estimation assures indeed this continuity, and not for Reuss estimation.

It should be noted that in the computation, the slip characteristic of the α_2-Ti_3Al is not considered in this preliminary study. The reason is that the critical resolved shear stress for the slip systems in γ-TiAl is lower than that for the slip systems in α_2-Ti_3Al. As a result, γ-TiAl plates always yield first and the α_2 lamellae do not deform at least at the early stage of the yielding of the PST crystal. Therefore, the α_2 lamellae always play a role as a strong barrier against propagation of the slip and/or twin through it. However,

with further deformation, the deformation of the α_2 lamellae must also play a role in controlling the behavior of the PST crystal. The large difference in the critical resolved shear stresses for the prismatic slip and the pyramidal slip of the α_2 lamellae [16] may contribute to the different strengthening effect for $\theta = 0°$ and $\theta = 90°$. These effects together with the strain hardening effect in the γ phase will be considered in a further report.

Conclusion

In this paper, we therefore propose an analytical approach based on a micromechanical method and dislocation theory to predict the yield stress of PST crystals. The detailed domain microstructures of the γ lamellae are taken into account. The results show that the constant strain assumption in the different variants of the γ phase gives better correlation with the experiment.

Acknowledgements

The authors acknowledge financial support for this work from The Nature Science Foundation of China under contract no. 5989150.

References

[1] Appel, F., & Wagner, R. (1998). Mater Sci Eng R22, 187.
[2] Dimiduk, D. M., Hazzledine, P. M., Parthasarathy, T. A., Seshagiri, S., & Mendiratta, M. G. (1998). Metall Mater Trans A 29A, 37.
[3] Yoo, M. H., & Fu, C. L. (1998). Metall Mater Trans A 29A, 49.
[4] Scholögl, S. M., & Fischer, F. D. (1997). Philos Mag A 75, 621.
[5] Fujiwara, T., Nakamura, A., Hosomi, M., Nishitani, S. R., Shrai, Y., & Yamaguchi, M. (1990). Philos Mag A 61, 591.
[6] Lebensohn, R., Uhlenhut, H., Hartig, C., & Mecking, H. (1998). Acta Mater 46, 4701.
[7] Grujicic, M., & Zhang, Y. (1999). Mater Sci Eng A265, 285.
[8] Kad, B. K., Dao, M., & Asaro, R. J. (1995). Philos Mag A 75, 567.
[9] Kad, B. K., Dao, M., & Asaro, R. J. (1996). Mat Res Soc Symp Proc 434, 141.
[10] Sun, Y. Q. (1998). Philos Mag A 77, 1107.
[11] Scholögl, S. M., & Fischer, F. D. (1997). Mater Sci Eng A 240, 790.
[12] Yoo, M. H., & Lu, C. L. (1994). Minerals, Metals and Materials Society (p. 94). Warrandale, PA.
[13] Hu, G. K. (1996). Int J Plasticity 12, 439.
[14] Wapole, L. J. (1969). J Mech Phys Solids 17, 235.
[15] Kawabata, T., Kanai, T., & Izumi, O. (1985). Acta Metall 33, 1355.
[16] Minonishi, Y. (1991). Philos Mag A 63, 1085.
[17] Kishida, K., Inui, H., & Yamaguchi, M. (1998). Philos Mag A 78, 1.